Supporting Information

Electric Fields Measurements Reveal the Pivotal Role of Cofactor-Substrate Interaction in Dihydrofolate Reductase Catalysis

Aduragbemi S. Adesina,[†#] Katarzyna Świderek,[‡#] Louis Y. P. Luk,[†] Vicent Moliner*[‡] and Rudolf K. Allemann[†]*

[†]School of Chemistry, Cardiff University, Park Place, Cardiff, CF10 3AT, United Kingdom
[‡]Departament de Química Física i Analítica, Universitat Jaume I, 12071 Castellón, Spain

Corresponding authors: allemannrk@cardiff.ac.uk and moliner@uji.es

EXPERIMENTAL DETAILS

Variants of EcDHFR and BsDHFR including EcDHFR C85A/C152S (subsequently referred to as cysteine free EcDHFR), EcDHFR C85A/C152S/S148P/T46C (EcDHFR S148P/T46C) and BsDHFR C73V/T46C (BsDHFR T46C) were characterized by circular dichroism spectroscopy and kinetic analysis. The data suggests that labeling this position with nitrile probe has negligible effects on enzyme kinetics as reported previously by others.[1]

Circular dichroism analysis

Structural characterisation of the enzymes was carried out with Applied Photophysics circular dichroism spectroscopy. Comparison of the molar ellipticity of the wild type enzymes with the variants reveals that introduction of the nitrile probe into the active site have negligible effects on their structures.

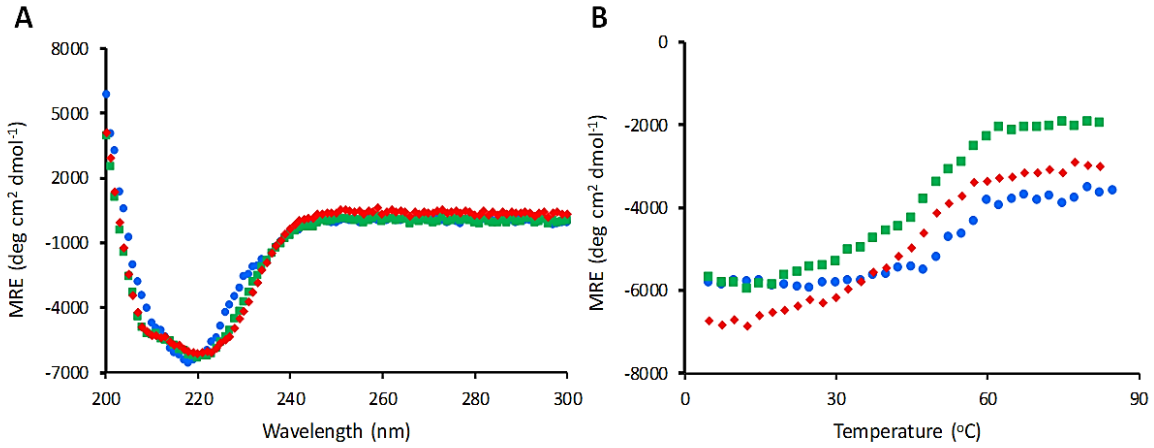

Figure S1. (A) CD spectra at 20 °C of cysteine free EcDHFR (blue), EcDHFR S148P/T46C (green) and EcDHFR S148P/T46C-CN (red) and (B) their thermal melting curves. CD spectra were recorded in 10 mM potassium phosphate buffer (pH 7.0) at a protein concentration of 10 µM.

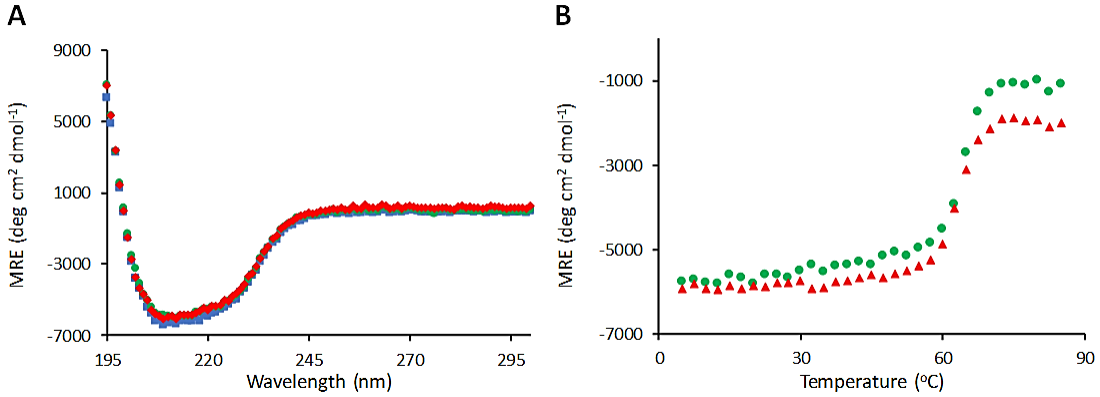

Figure S2. (A) CD spectra at 20 °C wild type BsDHFR (blue), BsDHFR T46C (green) and BsDHFR T46C-CN (red) and (B) thermal melting curves of the variant and its labeled counterpart. CD spectra were recorded in 10 mM potassium phosphate buffer (pH 7.0) at a protein concentration of 10 µM.

Kinetic analysis

Table S1. Kinetic parameters for EcDHFR variants and the nitrile labeled enzyme measured at pH 7.0 and 25 °C

Enzyme	k_{cat} (s^{-1})	K_M NADPH (μM)	K_M DHF (μM)	k_H (s^{-1})
EcDHFR cysteine-free*	9.4 ± 0.4	2.1 ± 0.1	0.8 ± 0.05	191 ± 6
EcDHFR S148P T46C	4.2 ± 0.3	4.7 ± 1.5	1.5 ± 0.2	53 ± 1
EcDHFR S148P T46C-CN	4.8 ± 0.3	2.4 ± 1.1	1.5 ± 0.3	59 ± 4

* data obtained from reference [2]

Table S2. Kinetic parameters for BsDHFR, its variant and the nitrile labeled enzyme measured at pH 7.0 and 20 °C

Enzyme	k_{cat} (s^{-1})	K_M NADPH (μM)	K_M DHF (μM)	k_H (s^{-1})
BsDHFR WT*	14.5 ± 1.2	127 ± 6	0.8 ± 0.05	102 ± 5
BsDHFR T46C	10.1 ± 1.2	121 ± 5	2.2 ± 0.4	61 ± 6
BsDHFR T46C-CN	12.1 ± 0.9	123 ± 6	1.9 ± 0.6	82 ± 5

* data obtained from reference [3]

Mass spectra analysis

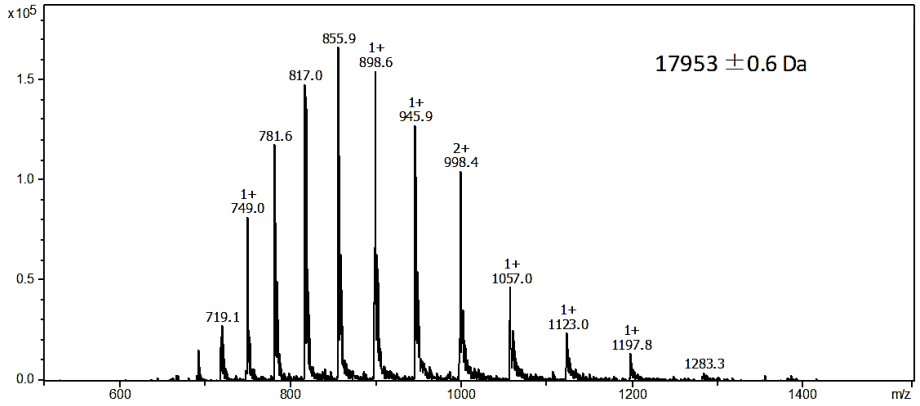

Figure S3. Charge envelope of EcDHFR T46C

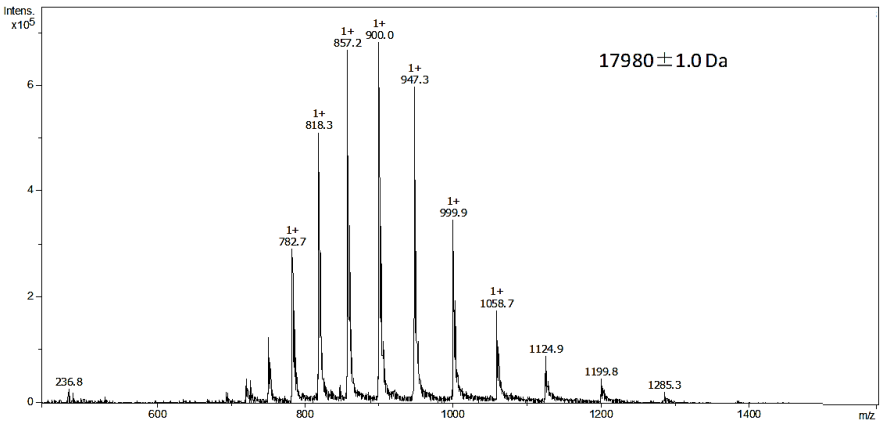

Figure S4. Charge envelope of EcDHFR T46C-CN

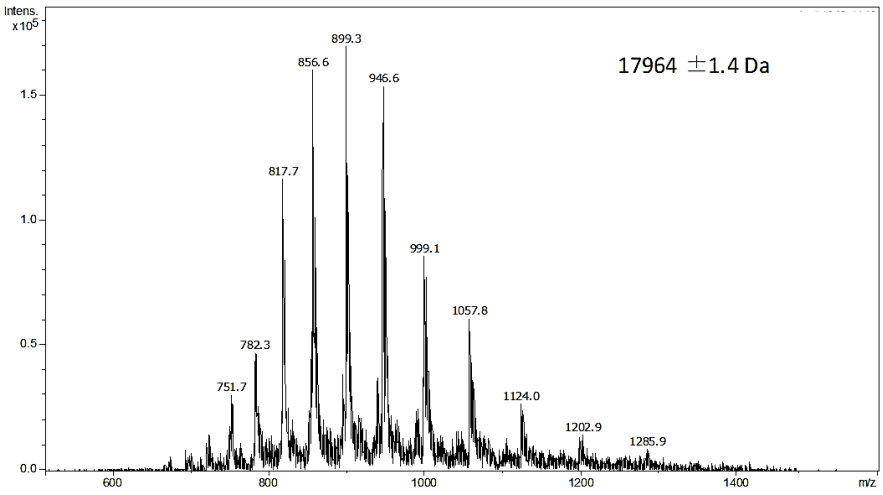

Figure S5. Charge envelope of EcDHFR S148P/T46C

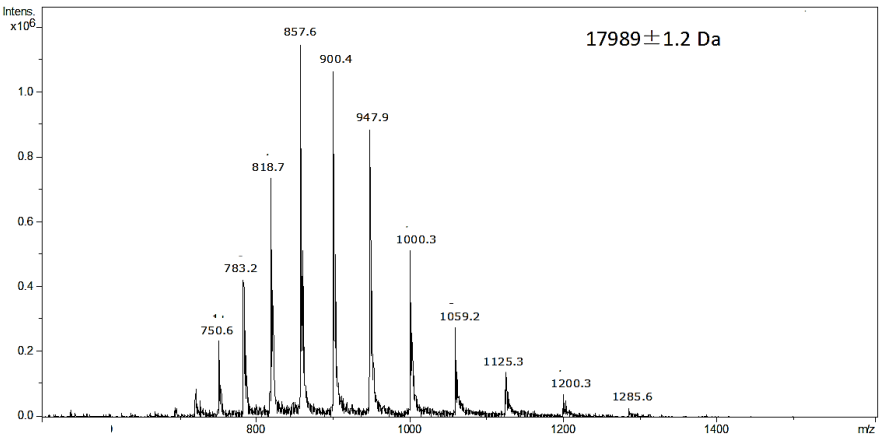

Figure S6. Charge envelope of EcDHFR S148P/T46C-CN

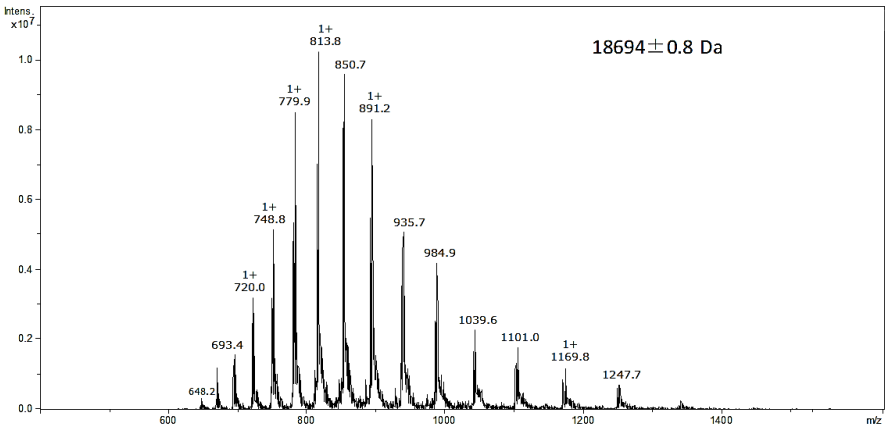

Figure S7. Charge envelope of BsDHFR T46C

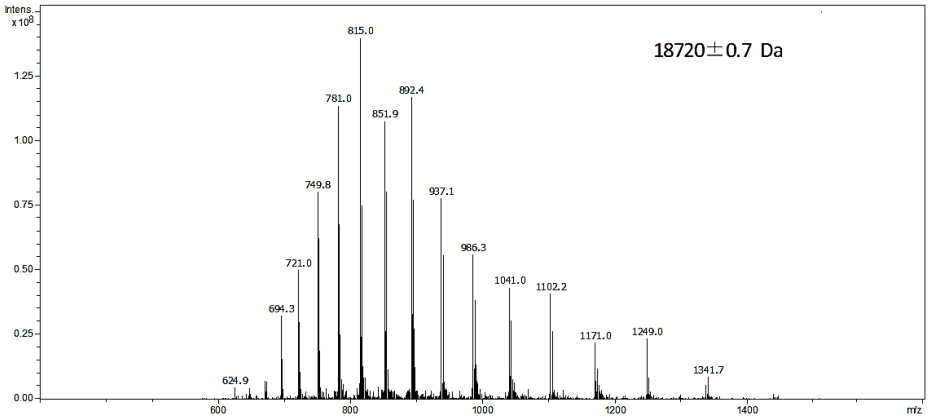

Figure S8. Charge envelope of BsDHFR T46C-CN

FTIR spectra data treatment

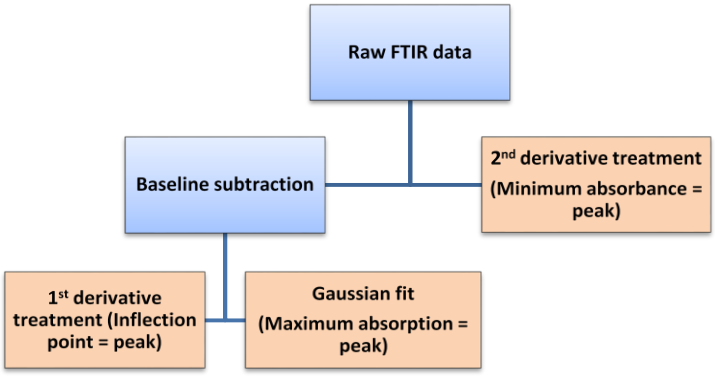

Figure S9. The scheme employed to determine the point of maximum absorbance of labeled DHFRs. Reported peaks were averages of the three data treatments (light brown boxes).

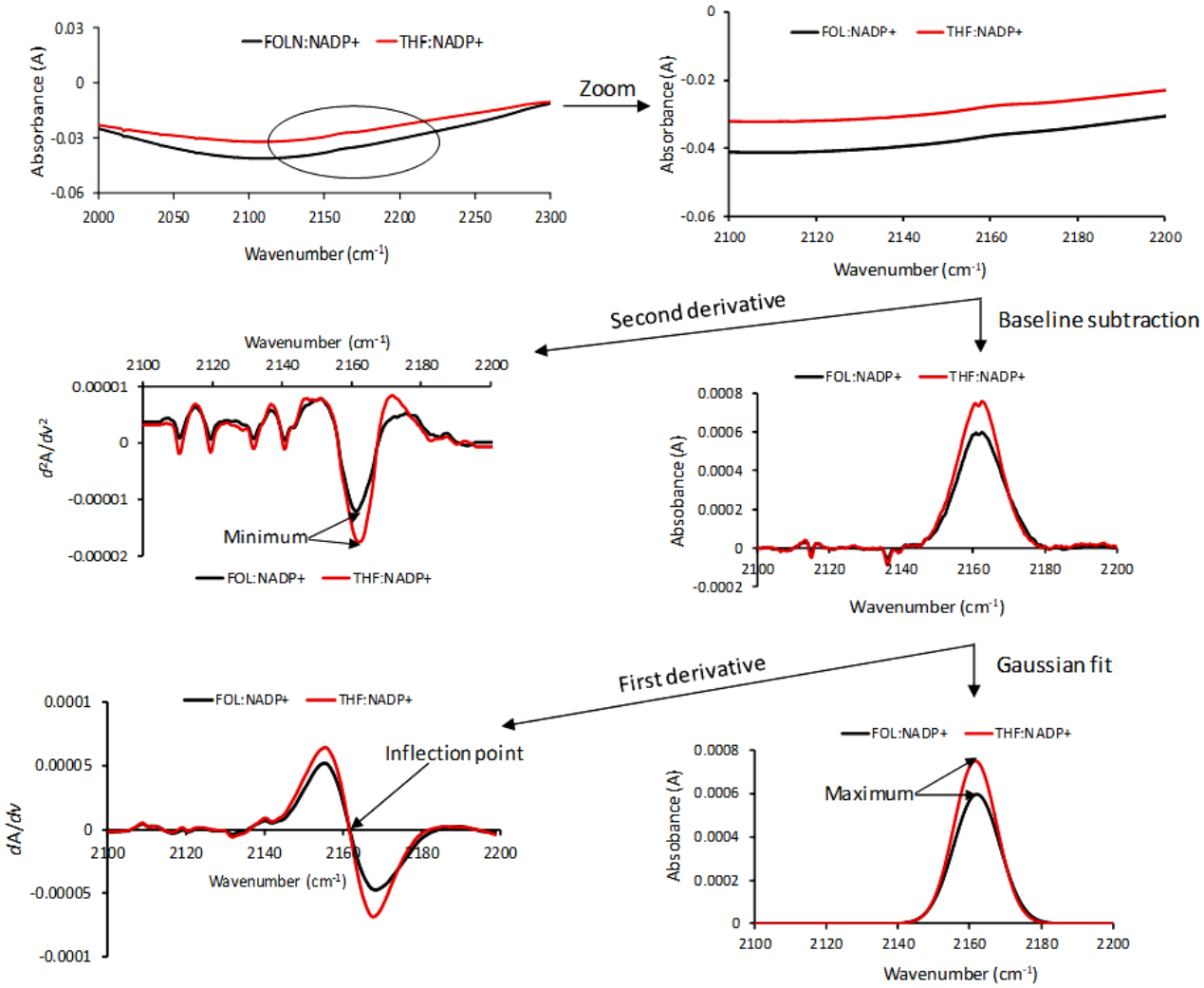

Figure S10. Graphical steps of spectra treatment employed for extracting the maximum vibrational frequency of labeled DHFRs. Reported peaks were averages of the three spectra treatments; minimum (2nd derivative), maximum (Gaussian fit), and inflexion point (1st derivative) from at least two independent measurements. Error is reported as the standard deviation of the treatments.

NMR spectra analysis

The NMR spectroscopy samples were prepared according to the previous report with 2.0 mM of S^{13}CN labeled protein, 10 mM ligands with 2.5 mM of 3-(trimethylsilyl)-1-propane sulfonic acid sodium salt as an external standard.[1]

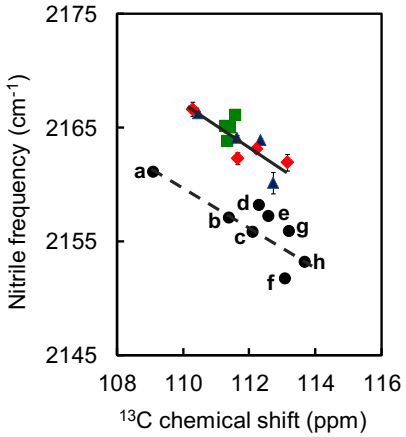

Figure S11. Calibration of hydrogen bonding interactions of the complexes of EcDHFR T46C-^{13}CN (triangles, dark blue) and EcDHFR S148P/T46C-^{13}CN (red diamond) and BsDHFR T46C-^{13}CN (square, green). Deviation of ~7 cm^{-1} from Stark calibration was observed. The Stark model is represented by the closed circle connected by the broken line,[1] indicating the fit for nitrile calibration in different solvents: a = cyclohexane, b = toluene, c = THF, d = chloroform, e = dichloromethane, f = dimethyl sulphoxide, g = acetone, and h = dimethylformamide, obtained from reference [4]

Table S3. Summary of ^{13}C NMR shifts, the vibrational frequency at maximum peak, and Full Width at Half Maximum (FWHM) values for the IR spectra in EcDHFR T46C, EcDHFR S148P/T46C and BsDHFR T46C determined at 20 °C

Enzymes	Complex	Vibrational frequency (cm^{-1})	FWHM (cm^{-1})	Chemical shifts (ppm)
EcDHFR T46C-CN	E	2164.1 ± 0.2	13.5 ± 0.2	111.6 ± 0.0
	E:NADPH	2166.2 ± 0.2	13.5 ± 0.0	110.5 ± 0.1
	E:$NADP^+$:folate	2163.9 ± 0.2	13.2 ± 0.1	112.4 ± 0.1
	E:$NADP^+$:THF	2160.1 ± 0.9	14.3 ± 0.1	112.7 ±0.0
	E:$NADP^+$	2164.6 ± 0.2	13.3 ± 0.2	n.d.
EcDHFR S148P/T46C-CN	E	2162.3 ± 0.5	13.1 ± 0.1	116.3 ± 0.1
	E:NADPH	2166.6 ± 0.6	14.5 ± 0.2	110.5 ± 0.1
	E:$NADP^+$:folate	2161.9 ± 0.7	12.1 ± 0.1	112.4 ±0.2
	E:$NADP^+$:THF	2163.1 ± 0.4	14.5 ± 0.2	112.7 ±0.2
	E:$NADP^+$	2165.2 ± 1.0	14.0 ± 0.1	n.d.
BsDHFR T46C-CN	E	2165.0 ± 0.6	15.9 ± 0.2	111.4 ± 0.1
	E:NADPH	2166.1 ± 0.4	16.6 ± 0.3	111.6 ± 0.2
	E:$NADP^+$:folate	2163.8 ± 0.2	17.2 ± 0.2	111.4 ± 0.0
	E:$NADP^+$:THF	2165.1 ± 0.7	14.4 ± 0.1	111.3 ± 0.1
	E:$NADP^+$	2165.5 ± 0.2	16.2 ± 0.2	n.d.

n.d. = not determined

COMPUTATIONAL DETAILS

Gas phase calculations

Geometry optimization and frequency calculations of the nitrile bond of MeCN and MeSCN were carried out with Gaussian09 package of programs in the gas phase with three semiempirical methods and 18 density functionals (Figure S12).[5] Frequency calculations were carried out with the harmonic and the anharmonic approximations, as reported in Table S4.

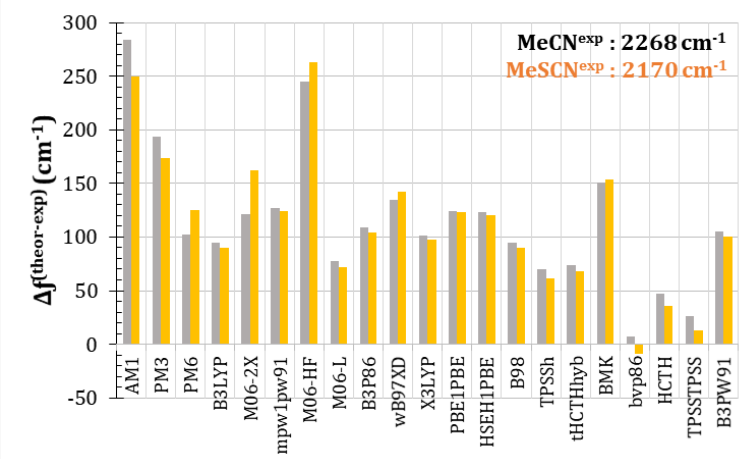

Figure S12. Difference between experimental and theoretically predicted nitrile bond frequency**.** 6-311++g(d,p) was the basis set for all the tested DFT methods.

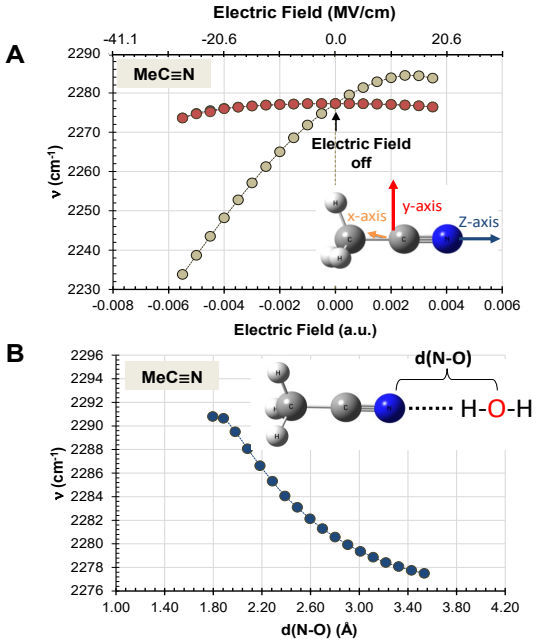

Figure S13. (A) Frequency of the nitrile bond of the MeCN molecule computed in the gas phase under the effect of external electric fields applied on the Z (grey points) and X (red points) directions. (B) The frequency of the nitrile bond of the MeCN molecule computed in the gas phase as a function of the distance of a hydrogen bond interaction with a water molecule. Electric field values are reported in a.u. (1 a.u. ≡ 5.14225 x 10^3 MV/cm).

Table S4. Frequency of the nitrile probe under the effect of an external electric field applied on the longitudinal direction of the bond, computed at BVP86/6-311++g(d,p) level with the harmonic ($\nu^{harmonic}$) and the anharmonic ($\nu^{anharmonic}$) approximations in the gas phase.

Z-axis $\vec{F}_{field}$ (a.u.)	$\nu^{harmonic}$ (cm^{-1})	$\nu^{anharmonic}$ (cm^{-1})	$\Delta\nu$ (cm^{-1})
0.0035	2283.747	2283.854	-0.11
0.0030	2284.339	2284.530	-0.19
0.0025	2284.439	2284.448	-0.01
0.0020	2283.823	2283.861	-0.04
0.0015	2282.802	2282.821	-0.02
0.0010	2281.350	2281.363	-0.01
0.0005	2279.492	2279.514	-0.02
0.0000	2277.283	2277.295	-0.01
-0.0005	2274.724	2274.722	0.00
-0.0010	2271.801	2271.812	-0.01
-0.0015	2268.569	2268.579	-0.01
-0.0020	2265.022	2265.038	-0.02
-0.0025	2261.239	2261.207	0.03
-0.0030	2257.095	2257.107	-0.01
-0.0035	2252.753	2252.765	-0.01
-0.0040	2248.203	2248.214	-0.01
-0.0045	2243.486	2243.496	-0.01
-0.0050	2238.659	2238.668	-0.01
-0.0055	2233.790	2233.798	-0.01

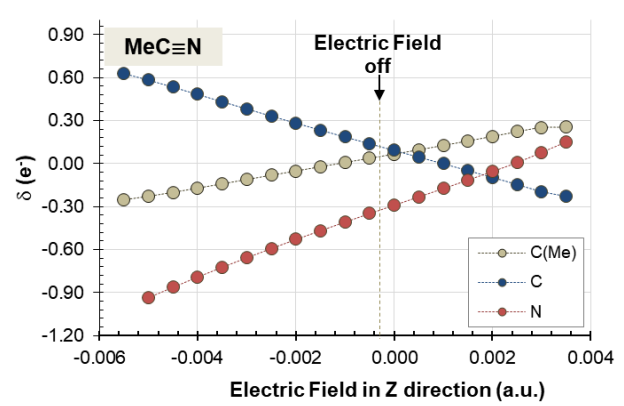

Figure S14. Atomic charges on the two carbon atoms and on the nitrogen atom of the MeCN molecule computed in the gas phase under the effect of external electric fields applied on the direction of the nitrile bond (Z direction).

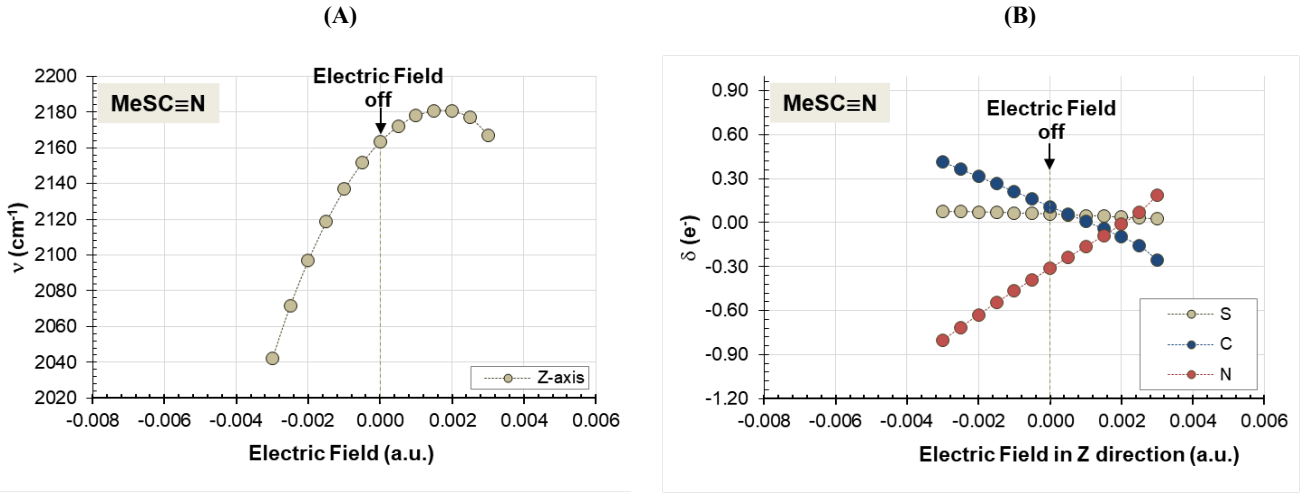

Figure S15. Frequency of the CN bond (A) and atomic charges on the sulphur, carbon and nitrogen atoms (B) of the MeSCN molecule computed in the gas phase under the effect of external electric fields applied on the direction of the nitrile bond (Z direction).

QM/MM calculations

System Preparation

The calculations of the closed Michaelis complex, E:NADP$^+$:folate of EcDHFR were carried out from the initial X-ray structures as deposited in the PDB with code 4P66. This structure contains a nitrile probe (XCN) attached at position 46, as well as C85A, D37N, and C152S mutations. NADP$^+$ and MTX (methotrexate) were in the active site. MTX was manually modified to FOL (NA4 mutated to O4, and CM removed). The missing side chain for Glu17, Asn18, Asn23, Arg33, Arg52, Gln108 and Glu118 where added.

The protonation states of titratable residues were determined with PROPKA ver. 3.0 3.[6] Accordingly, His149 was protonated in δ position, His124 in ε position and His 45, 114 and 141 in both δ and ε positions. The hydrogen atoms were then added considering pH 7 with the utilities of fDYNAMO library.[7] Finally, the system was solvated by placing it in a 100 × 80 × 80 Å^3 pre-equilibrated box of water molecules. Any water with an oxygen atom lying in a radius of 2.8 Å from a heavy atom of the protein was deleted. The geometry of the system was optimized applying a series steepest descent conjugated gradient minimization (gradient tolerance of 5 kJ·mol^{-1}·Å^{-1}) followed by a series of L-BFGS-B (gradient tolerance of 0.1 kJ·mol^{-1}·Å^{-1}). A truncation function (shift function) was applied to treat the non-bonded interactions, with an internal cut-off of 14.5 Å and an external of 16 Å. All the optimization algorithms were implemented in the fDYNAMO library. Then, 5 ns of classical MD simulations were run to equilibrate the system with AMBER force field,[8] as implemented in NAMD software.[9] Parameters for both substrates obtained with Antechamber[10] at AM1 level. Time evolution of the RMSD on the 5 ns of classical MM molecular dynamics simulation in the Michaelis complex (E:NADP$^+$:folate) is displayed in Figure S16B, while B-factor of the backbone after the 5 ns of classical MM molecular dynamics simulation is shown in Figure S17.

In the case of the preparation of the occluded product ternary complex, E:NADP$^+$:THF, the initial structure was obtained from PDB 1RX6. In this case, the three mutations have been introduced: C85A/C152S/T46SCN + D37N (names of last atoms in SCN SG-CSNC). The active site contains NADP$^+$ and DDF (5,10-dideazatetrahydrofolic acid). This later was modified to THF (C10 mutated to N10; C5 mutated to N5) while the missing ring was added in the NADP$^+$. Same as in the closed conformation, the protonation state of the titratable residues of the EcDHFR was determined with PROPKA ver. 3.0 3. Accordingly, His149 was protonated in δ position, His124 in ε position and His 45, 114

and 141 in both δ and ε positions. Once the full protein was prepared, it was solvated using the same procedure as in the closed conformation and, after the same series of optimization algorithms, 5 ns of classical MM MD simulation was carried out. The time evolution of the RMSD on this occluded conformation is displayed in Figure S16C, while B-factor of the backbone after the 5 ns of classical MM molecular dynamics simulation is shown in Figure S17.

Finally, the holoenzyme binary complex, E: NADPH, was prepared from the closed Michaelis complex, E:$NADP^+$:folate, by removing the substrate and running the corresponding 5 ns of classical MD simulations for equilibration. The time-dependent evolution of the RMSD is displayed in Figure S16A.

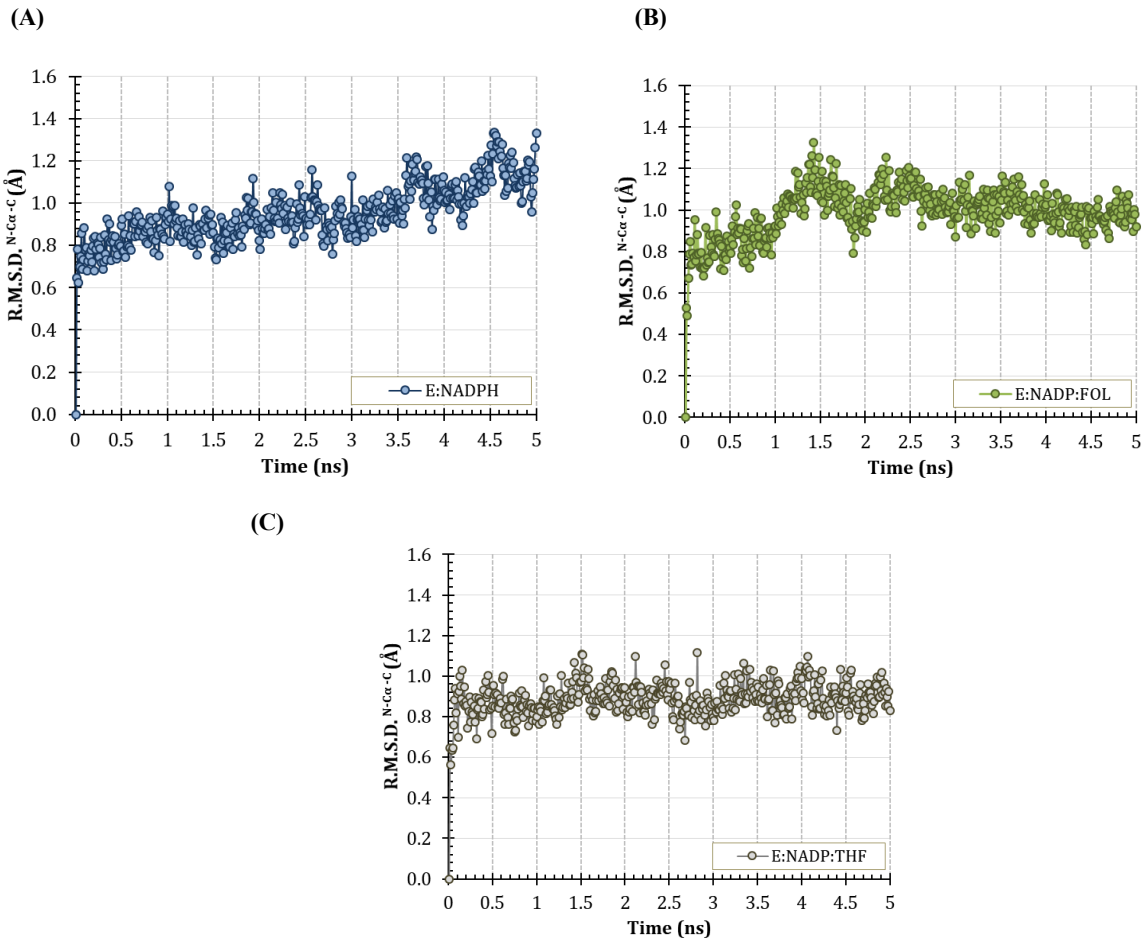

Figure S16. Time evolution of the RMSD on the 5 ns of classical MM molecular dynamics simulation on different complexes of EcDHFR: (A) the holoenzyme E:$NADP^+$ (B) Michaelis complex, E:$NADP^+$:folate and (C) the product ternary complex, E:$NADP^+$:THF.

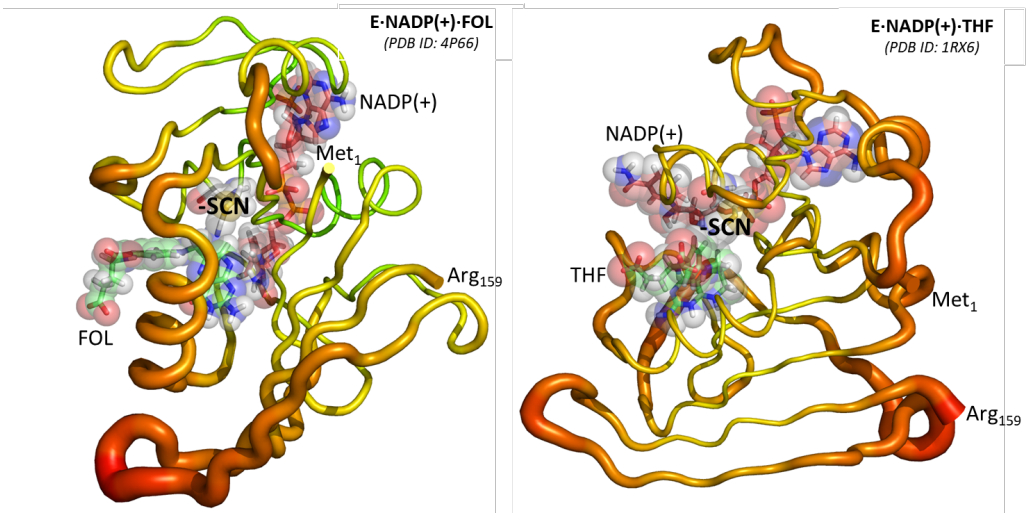

Figure S17. B-factor of the backbone after the 5 ns of classical MM molecular dynamics simulation on the closed Michaelis complex, E:NADP$^+$:folate (left) and on the product ternary complex, E:NADP$^+$:THF (right).

Nitrile frequency calculations.

In order to carry out the frequency determination of the nitrile bond, 500 structures were randomly selected from the last 500 ps of the classical MD simulations. Then, a hybrid quantum mechanics/molecular mechanics (QM/MM) scheme was used, where the probe was described by BVP86 functional with the standard 6-311++g(d,p) basis set, and the rest of the protein and water molecules with OPLS-AA[11] and TIP3P[12] classical force fields, respectively. A detail of the active site showing the QM/MM partition is presented in Figure S18.

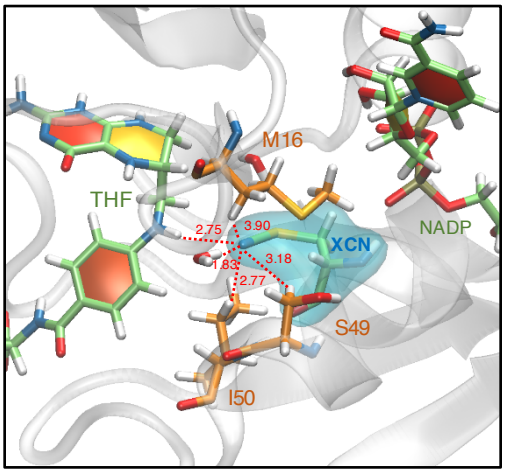

Figure S18. Snapshot of the active site of EcDHFR in the Michaelis complex, E:NADP$^+$:folate after 5 ns of MM MD simulations. Atoms in the blue area are those included in the QM region. A quantum hydrogen link atom was added between the Cα and Cβ atoms of the XCN residue.

Quantification of the hydrogen bond interactions

The contributions of H-bond interactions between the nitrile group of the probe and the active site of the EcDHFR in both states were computed according to the geometrical distance and angle function of equation S1, as proposed by Jensen and co-workers.[13]

Equation (S1)

Distance contribution:

$$HB_{dist} = \begin{cases} D - d_2 & if\ D \leq d_2 \\ 0 & if\ d_2 < D \end{cases}$$

d_2 = 3.0 Å used to compute H-bond contribution

Angle and distance contribution:

$$HB_{dist/angle} = \begin{cases} -cos\theta \cdot (D - d_2) & if\ D \leq d_2,\ \theta > 90° \\ 0 & if\ d_2 < D,\ \theta \leq 90° \end{cases}$$

A.

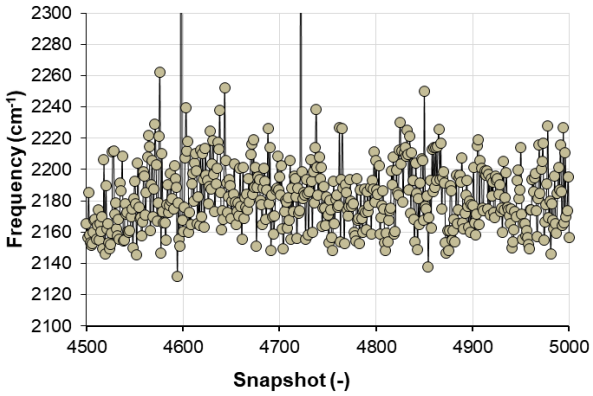

B.

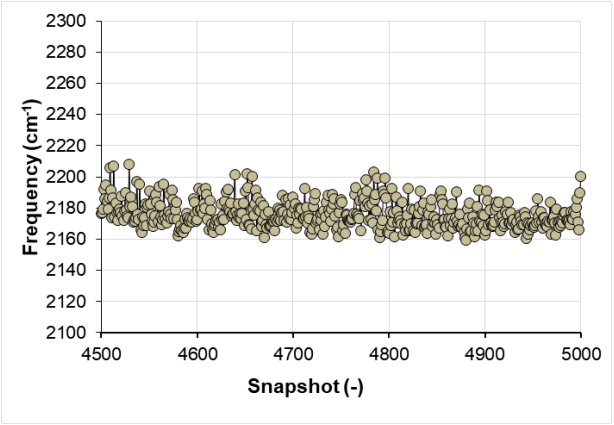

C.

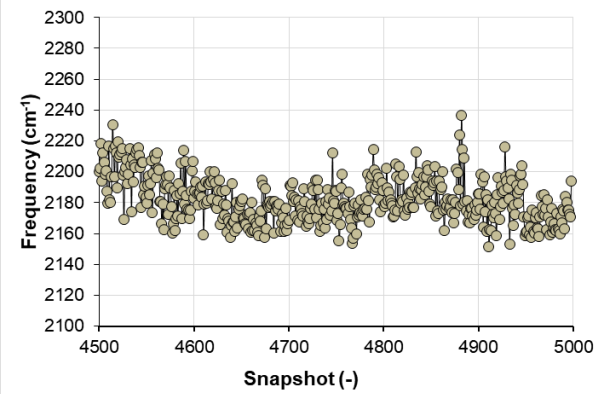

Figure S19. Time evolution of the nitrile frequency on the 5 ns of classical MM molecular dynamics simulation on different complexes of EcDHFR: (A) the holoenzyme, E:NADPH; (B) Michaelis complex, E:NADP$^+$:folate; and (C) the product ternary complex, E:NADP$^+$:THF.

Table S5. QM/MM theoretical calculation of the frequency of the nitrile bond (ν), total electric field projected on the nitrile bond ($\vec{F}_{all}$) and its contributions coming from the cofactor ($\vec{F}_{NADP}$). Values averaged over structures selected from the last 51 ps of the full classical MD simulations. The hydrogen bond interactions (HB) were quantified on representative structures using equation S1.

EcDHFR complex	**ν (cm^{-1})**	$\vec{F}_{all}$ **(a.u.)**	$\vec{F}_{NADP}$ **(a.u.)**	**H.B (a.u.)**
E:NADPH	2180.0 ± 21.1	-0.0152 ± 0.0033	-0.0076 ± 0.0010	1.49
E:NADP$^+$:folate	2173.6 ± 6.6	-0.0024 ± 0.0034	-0.0082 ± 0.0013	0.49
E:NADP$^+$:THF	2169.8 ± 13.5	-0.0077 ± 0.0035	-0.0068 + 0.0005	0.72

REFERENCES:

(1) Liu, C. T.; Layfield, J. P.; Stewart, R. J.; French, J. B.; Hanoian, P.; Asbury, J. B.; Hammes-Schiffer, S.; Benkovic, S. J. Probing the Electrostatics of Active Site Microenvironments along the Catalytic Cycle for Escherichia Coli Dihydrofolate Reductase. *J. Am. Chem. Soc.* **2014**, *136*, 10349–10360.

(2) Tey, L.-H.; Loveridge, E. J.; Swanwick, R. S.; Flitsch, S. L.; Allemann, R. K. Highly Site-Selective Stability Increases by Glycosylation of Dihydrofolate Reductase. *FEBS J.* **2010**, *277*, 2171–2179.

(3) Guo, J.; Luk, L. Y. P.; Loveridge, E. J.; Allemann, R. K. Thermal Adaptation of Dihydrofolate Reductase from the Moderate Thermophile Geobacillus Stearothermophilus. *Biochemistry* **2014**, *53*, 2855–2863.

(4) Fafarman, A. T.; Sigala, P. A.; Herschlag, D.; Boxer, S. G. Decomposition of Vibrational Shifts of Nitriles into Electrostatic and Hydrogen-Bonding Effects. *J. Am. Chem. Soc.* **2010**, *132*, 12811–12813.

(5) Frisch, M. J.; Trucks, G. W.; Schlegel, H. B.; Scuseria, G. E.; Robb, M. A.; Cheeseman, J. R.; Scalmani, G.; Barone, V.; Mennucci, B.; Petersson, G. A.; Nakatsuji, H.; Caricato, M.; Li, X.; Hratchian, H. P.; Izmaylov, A. F.; Bloino, J.; Zheng, G.; Sonnenberg, J. L.; Hada, M.; Ehara, M.; Toyota, K.; Fukuda, R.; Hasegawa, J.; Ishida, M.; Nakajima, T.; Honda, Y.; Kitao, O.; Nakai, H.; Vreven, T.; Montgomery, J.A., J.; Peralta, J. E.; Ogliaro, F.; Bearpark, M.; Heyd, J. J.; Brothers, E.; Kudin, K. N.; Staroverov, V. N.; Kobayashi, R.; Normand, J.; Raghavachari, K.; Rendell, A.; Burant, J. C.; Iyengar, S. S.; Tomasi, J.; Cossi, M.; Rega, N.; Millam, N. J.; Klene, M.; Knox, J. E.; Cross, J. B.; Bakken, V.; Adamo, C.; Jaramillo, J.; Gomperts, R.; Stratmann, R. E.; Yazyev, O.; Austin, A. J.; Cammi, R.; Pomelli, C.; Ochterski, J. W.; Martin, R. L.; Morokuma, K.; Zakrzewski, V. G.; Voth, G. A.; Salvador, P.; Dannenberg, J. J.; Dapprich, S.; Daniels, A. D.; Farkas, Ö.; Foresman, J. B.; Ortiz, J. V.; Cioslowski, J.; Fox, D. J. Gaussian 09. Gaussian, Inc.,: Wallingford CT, **2009**.

(6) Olsson, M. H. M.; Søndergaard, C. R.; Rostkowski, M.; Jensen, J. H. PROPKA3: Consistent Treatment of Internal and Surface Residues in Empirical PK a Predictions. *J. Chem. Theory Comput.* **2011**, *7*, 525–537.

(7) Field, M. J.; Albe, M.; Bret, C.; Martin, F. P.; Thomas, A. The Dynamo Library for Molecular Simulations Using Hybrid Quantum Mechanical and Molecular Mechanical Potentials. *J. Comput. Chem.* **2000**, *21*, 1088–1100.

(8) Zhang, W. E. I.; Yang, R.; Cieplak, P.; Luo, R. A. Y.; Lee, T.; Caldwell, J.; Wang, J.; Kollman, P. A Point-Charge Force Field for Molecular Mechanics Simulations of Proteins Based on Condensed-Phase. *J. Comput. Chem.* **2003**, *24*, 1999–2012.

(9) Phillips, J. C.; Braun, R.; Wang, W. E. I.; Gumbart, J.; Tajkhorshid, E.; Villa, E.; Chipot, C.; Skeel, R. D.; Poincare, H. Scalable Molecular Dynamics with NAMD. *J. Comput. Chem.* **2005**, *26*, 1781–1802.

(10) Wang, J.; Wang, W.; Kollman, P. A.; Case, D. A. Automatic Atom Type and Bond Type Perception in Molecular Mechanical Calculations. *J. Mol. Graph. Model.* **2006**, *25*, 247–260.

(11) Jorgensen, W. L.; Maxwell, D. S.; Tirado-Rives, J. Development and Testing of the OPLS All-Atom Force Field on Conformational Energetics and Properties of Organic Liquids. *J. Am. Chem. Soc.* **1996**, *118*, 11225–11236.

(12) Jorgensen, W. L.; Chandrasekhar, J.; Madura, J. D.; Impey, R. W.; Klein, M. L. Comparison of Simple Potential Functions for Simulating Liquid Water. *J. Chem. Phys.* **1983**, *79*, 926–935.

(13) Li, H.; Robertson, A. D.; Jensen, J. H. Very Fast Empirical Prediction and Rationalization of Protein PKa Values. *Proteins Struct. Funct. Bioinforma.* **2005**, *61*, 704–721.